An automated cell viability quantification method for low-resolution confocal images of closely packed cells based on a modified gradient flow tracking algorithm

Article *in* Journal of Microscopy · November 2015

DOI: 10.1111/jmi.12322

CITATIONS
3

READS
141

4 authors, including:

Rosa Kaviani
McGill University
9 PUBLICATIONS **34** CITATIONS
SEE PROFILE

Pooya Merat
McGill University
7 PUBLICATIONS **12** CITATIONS
SEE PROFILE

Florina Moldovan
CHU Sainte-Justine
116 PUBLICATIONS **2,471** CITATIONS
SEE PROFILE

Journal of
Microscopy

Journal of Microscopy, Vol. 261, Issue 3 2016, pp. 217–226 doi: 10.1111/jmi.12322
Received 7 October 2014; accepted 31 August 2015

An automated cell viability quantification method for low-resolution confocal images of closely packed cells based on a modified gradient flow tracking algorithm

R. KAVIANI*,†, P. MERAT‡, F. MOLDOVAN†,§ & I. VILLEMURE*,†
*Department of Mechanical Engineering, Ecole Polytechnique of Montreal, Montreal, Canada
†Research Center, Sainte-Justine University Hospital, Montreal, Canada
‡Department of Electrical and Computer Engineering, McGill University, Montreal, Canada
§Department of Dental Medicine, University of Montreal, Montreal, Canada

Key words. Convergence centers, gradient flow tracking, live/dead labelling, viability quantification.

Summary

Fluorescent-based live/dead labelling combined with fluorescent microscopy is one of the widely used and reliable methods for assessment of cell viability. This method is, however, not quantitative. Many image-processing methods have been proposed for cell quantification in an image. Among all these methods, several of them are capable of quantifying the number of cells in high-resolution images with closely packed cells. However, no method has addressed the quantification of the number of cells in low-resolution images containing closely packed cells with variable sizes. This paper presents a novel method for automatic quantification of live/dead cells in 2D fluorescent low-resolution images containing closely packed cells with variable sizes using a mean shift-based gradient flow tracking. Accuracy and performance of the method was tested on growth plate confocal images. Experimental results show that our algorithm has a better performance in comparison to other methods used in similar detection conditions.

Introduction

The measurement of cell viability is critical in many areas of biomedical research such as pharmaceutics, tissue engineering and mechanobiology. Cell viability can be determined using several methods: proliferation assays, functional assays (cells metabolic activities such as MMT), DNA labelling by fluorescent probes, observation of morphological changes of cells and finally, membrane integrity tests, which use a combination of a membrane-permeable dye (to stain viable cells) and a membrane-impermeable DNA-binding molecule (to stain dead cells; Park *et al.*, 2000; Stoddart, 2011). Cell viability quantification can be completed using microscopic observation followed by counting, biochemical methods using colorimetry or by flow cytometry using specific antibodies. Although flow cytometry and colorimetry result in quantitative viability information, they do not provide information on the location-dependent viability in different tissue zones, and can only be performed on cell samples (Godfrey *et al.*, 2005). Conversely, microscopy can be performed both on cells samples and tissue sections, with the advantage of providing the exact live/dead cells location, but it is not a quantitative method.

Among the existing methods for viability evaluation, membrane integrity tests and fluorescent probes have the advantage of being nonradioactive, and of being neither dependent on cell proliferation nor metabolic activity (Gantenbein-Ritter *et al.*, 2011). Moreover, results of these tests, which can be visualized using fluorescent microscopes, are perfectly suited for applications such as mechanobiology and tissue engineering, where not only the severity of cell damage is important but also the location of the damage is of interest. One of the widely used methods among fluorescent probes is the live/dead viability kit, which combines Calcein AM and Ethidium Homodimer 1 stains. Calcein AM stains live cells based on the esterase activity in the cell cytoplasm, which then produces an intense uniform green fluorescence. Ethidium Homodimer 1 is attached to the DNA of cells with compromised membrane, which results in a red staining of the nucleus of dead cells (Spaepen *et al.*, 2011). The commonly used method for evaluating the number of dead/live cells in the resulting fluorescent images is manual counting (MC). However, this approach is time-consuming and can be subjective with intra- and interindividual variations.

Correspondence to: Isabelle Villemure, Department of Mechanical Engineering, École Polytechnique de Montréal, P.O. Box 6079, Station Centre-Ville, Montreal, QC, H3C 3A7, Canada. Tel: (514)340-4711; fax: (514)340-4176; e-mail: isabelle.villemure@polymtl.ca

Recently, many image analysis approaches have been implemented for automatic cell quantification in fluorescent images. These approaches can be categorized in two general groups. Methods of the first category use information of image intensity for segmentation. Several methods, such as thresholding (Xiong *et al.*, 2006), watershed transformation (Malpica *et al.*, 1997) or Hough transform (Guan & Yan, 2011) have been previously proposed in this category. Simple thresholding does not work properly on noisy or uneven illuminated images or when contrast between cells and background is not uniform throughout the image. However, adaptive thresholding (Chan *et al.*, 2012) can overcome contrast problems and successfully identify scattered cells but it fails to adequately segment closely packed cells, such as proliferative chondrocytes found in the growth plates, where cell clusters are segmented as one object. To overcome this problem, watershed algorithm, which is a morphological algorithm, has been used to segment overlapping cells (Malpica *et al.*, 1997). However, this method is very sensitive to the choice of image transformation or initial markers and can easily lead to incorrect or oversegmentation. Hough transform is a feature extraction method but it is mainly limited to segmentation of circular cells (Guan & Yan, 2011). Another method for segmentation of convex round objects referred to as dots was introduced by Bernardis & Yu (2010). This method is a spectral graph cut algorithm based on the attraction and repulsion between pixels, computed from local intensity distribution. This method is successful in identifying convex objects of different sizes in many types of images. However, it has not been tested on low-resolution images. Other methods, based on mean shift (MS) algorithm, have also been used for detection of object centers in images (Collins, 2003; Yang *et al.*, 2006), but it is not clear whether these mean shift-based methods perform as well in low- and high-resolution images containing closely packed cells of different sizes and shapes.

Methods from the second category use gradient information of the images. In this category, convergence index (CI) filtering methods, such as sliding band filter (SBF) and Iris filters (IF), can segment closely packed cells with round shapes and are insensitive to contrast of the images (Quelhas *et al.*, 2010; Esteves *et al.*, 2012; Nam *et al.*, 2012; Sui & Wang, 2013). These methods work well for low-resolution images (Sui & Wang, 2013); however, it is not clear if they can identify cells with different shapes and sizes. Other methods in this category use iterative voting along the gradient direction followed by mean shift (Parvin *et al.*, 2007, Qi *et al.*, 2012). Performing the voting enhances the performance of the method in comparison to the mean shift. These methods give satisfactory results in finding subcellular members, and cell centers in high-resolution images; however, their performance on low-resolution images has not been tested yet. Another successful method in segmenting overlapping cells was proposed by Li *et al.* (2008). This method uses gradient flow tracking (GFT) on a diffused gradient vector of the image to find cell centers (Li *et al.*, 2008).

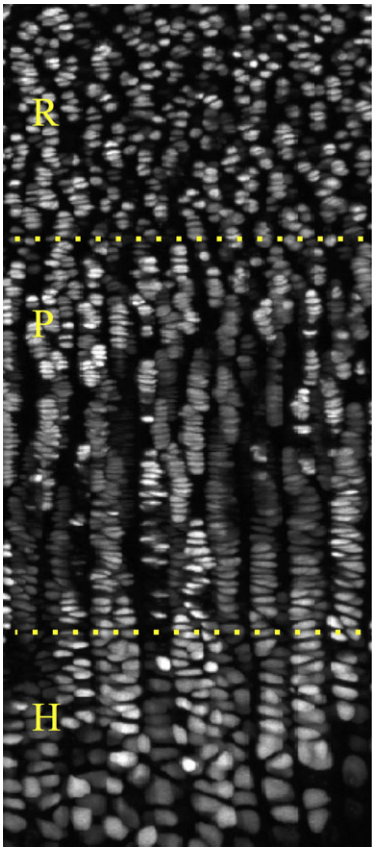

Fig. 1. Three growth plate zones: reserve (R), proliferative (P), hypertrophic (H).

However, the algorithm is sensitive to local changes in the intensity and, as a result, it uses smoothing with large kernel size to smooth cell textures, which is not desirable when cells are too close.

Since in confocal images cells usually have convex shapes and thus their surrounding gradient vectors point towards their centers (Kobatake & Hashimoto, 1999), using a method for tracking the gradient flow seems logical. Hence, the primary goal of this paper was to implement and validate a robust and simple GFT image-processing method-based on MS algorithm for quantifying the number of live and dead cells in low-resolution live/dead labelled fluorescent images containing closely packed cells with different sizes and shapes. Unlike the method of Li *et al.* (2008), our method does not use a diffusion model for diffusing the gradient on the image and it uses the normalized gradient vector field. Similar to the MS algorithm, our method is iterative and in each iteration, the centers of kernels are shifted to a new position estimated based on the gradient data of their neighbourhood. The paper is organized as follows. Material and Methods section introduces the data used in our experiments as well as the technique developed for quantifying the number of cells in fluorescent images. In Result and Discussion sections, obtained results

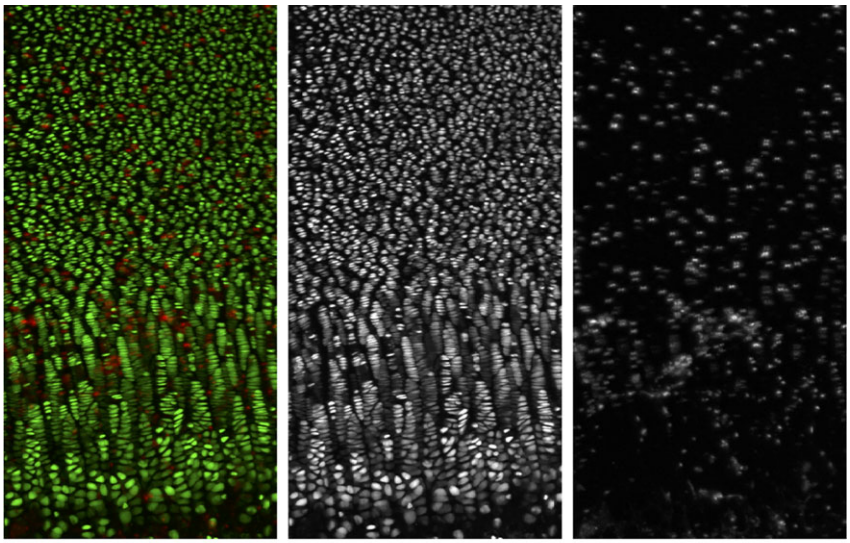

Fig. 2. Confocal images of live (green channel) and dead (red channel) cells from a growth plate tissue.

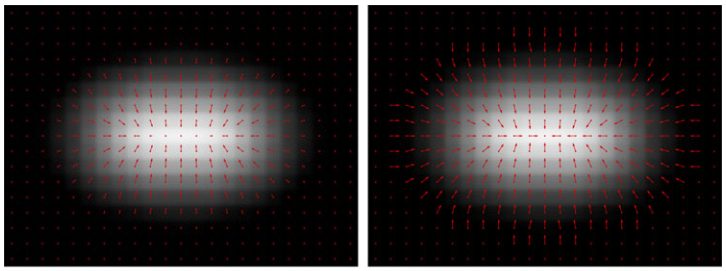

Fig. 3. Intermediate difference gradient vectors of a convex shape.

using the developed method, the Iris filter, the gradient tracking method, mean shift, the single pass voting algorithm and manual counting are compared and discussed, respectively. Finally, the conclusive remarks are presented in Conclusion section.

Materials and Methods

Tissue preparation and image acquisition

In this paper, growth plate confocal images with three different shapes and sizes of cells located in the three different zones (hypertrophic (H), proliferative (P) and reserve (R)) have been used (Fig. 1). Growth plate cylindrical explants (n = 15) were extracted from distal ulnae of 4-week-old swines within 2 hours of slaughter. A 1-mm-thick section was harvested from the central part of each explant and stained using a solution of 1 μM Calcein Am (Molecular Probes, Invitrogen, Montreal, Canada) and 2 μM Ethidium Homodimer 1 (Molecular Probes, Invitrogen) for 30 min at 37°C. Sections were

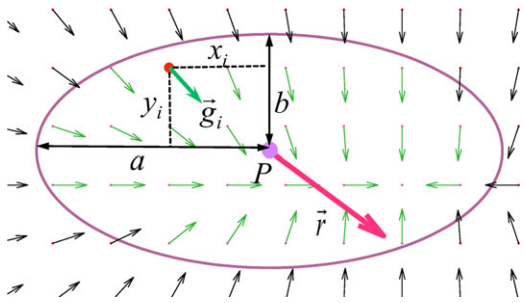

Fig. 4. Resultant vector for particle P.

washed in Hank's balanced salt solution (HBSS, Life Technologies, Invitrogen, Montreal, Canada) three times for 3 min. A 100-μm-thick image spanning the three zones of the growth plate was taken from serial sections of 1024 × 1024 pixels using stacks of z-series (serial optical sections of 10 um). An inverted laser scanning confocal microscope (LSM 510, Carl Zeiss, Jena, Germany) was used for imaging. Images were collected using a 10 × 0.30 NA Plan-Neofluar lens (Carl Zeiss Inc.,

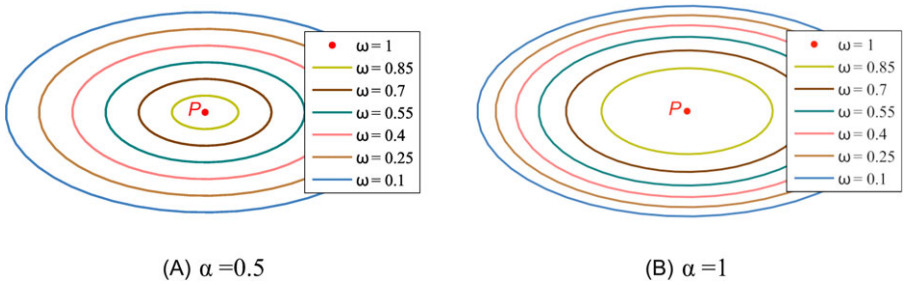

Fig. 5. Weight contours in the vicinity area of P.

Germany). The 488 nm line of an Argon laser was used for Calcein AM excitation combined with a band-pass 500–550 and the 543 nm line of a He–Ne laser was used for Ethidium Homodimer 1 excitation together with a low-pass 560 filter (Fig. 2). Maximum projection was used to obtain a planar 2D image of the cells. Following acquisition, an 800 × 400 region of interest was extracted from each image for quantification of live and dead cells. A Gaussian 2D filter with a kernel size of 3 and $\sigma = 0.5$ was applied on both channels of all images in the data set for smoothing image noises prior to applying any other algorithm on them. This kernel size was chosen considering the proximity of cells, especially in the proliferative zone of the growth plate.

Cell counting algorithm

In fluorescent images, cells usually have convex shapes and thus all the surrounding gradient vectors point towards their centers (Kobatake & Hashimoto, 1999). The method proposed herein is based on this concept and perform the gradient flow tracking using an algorithm similar to mean shift in order to detect cell centers. The image gradient can be calculated using an arbitrary method such as Sobel, Prewitt, central or intermediate difference (Gonzalez & Woods, 2002). In this paper, the intermediate difference method was used for calculating image gradients. The *Gradient vector field* is a vector representation of an image gradient (Fig. 3A). In the normalized gradient vector field, all vectors have unit length, except those corresponding to a zero gradient (Fig. 3B). In our proposed method, the normalized gradient vectors were used.

For a point (P) inside a normalized gradient vector field, an elliptical vicinity area is considered around P with semiaxes of dimensions a and b (Fig. 4). Using Eq. (1), a weighted resultant vector ($\vec{r}$) can also be defined for P, as a function of the normalized gradient vectors inside its vicinity area

$$\vec{r} = \sum_{i=1}^{n} \omega_i \overrightarrow{g_i}, \qquad (1)$$

where n is the number of gradient vectors inside the vicinity area of P and ω_i is the scalar weight coefficient of the i^{th} gradient vector $\overrightarrow{g_i}$. The weight coefficient ($0 \leq \omega_i \leq 1$) is a function of the relative position of $\overrightarrow{g_i}$ to P and is calculated by Eq. (2)

$$\omega_i = 1 - \left[\left(\frac{x_i - x_0}{a} \right)^2 + \left(\frac{y_i - y_0}{b} \right)^2 \right]^{\alpha}, \qquad (2)$$

where $\alpha > 0$ is a positive arbitrary exponent. Figure 5 shows weight contours for $\alpha = 0.5$ and $\alpha = 1$. Through an iterative process, each point moves along its momentary resultant vector. This displacement is equal to the resultant vector magnitude multiplied by a simulation step coefficient (C_{ss}) Eq. (3). The resultant vector changes at each iteration because of the displacement of vicinity area of the point

$$x_n = x_{n-1} + \vec{r} \times C_{ss}. \qquad (3)$$

Eventually, either each point will rest at some equilibrium position (first case), i.e. where the resultant vector is less than a limit (minimum point movement) or the maximum number of iterations will be reached and yet the resultant vector is not zero (second case). The points of the second case are then discarded in our further calculations. The equilibrium position of the points of the first group can then be considered as a possible cell centers. Figure 6 shows trajectory of a point from its initial position ($P_{(i)}$) to its equilibrium position ($P_{(f)}$) based

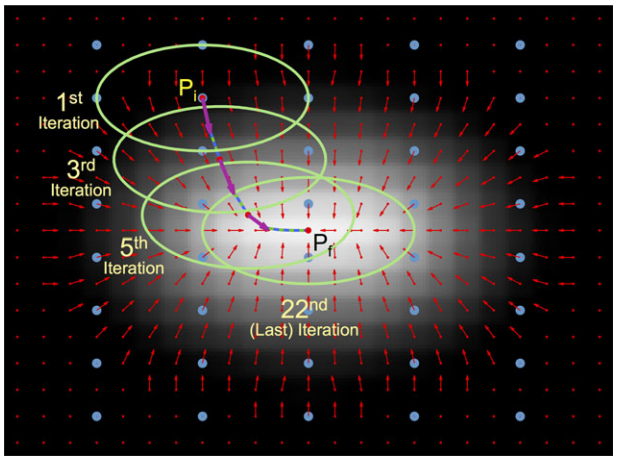

Fig. 6. Four snapshots of the vicinity area and resultant vectors along a sample trajectory.

on its momentary resultant vector along the trajectory. In this sample simulation, $\alpha = 1$ which was chosen by trial and error and the vicinity area is an ellipse with semiaxes of 4 and 2 similar to the size of the cell.

The algorithm first distributes a grid of points on the image and then calculates their final positions by repeating the aforementioned iterative simulation for each point. Afterwards, points closer than a certain distance (Merging-Threshold) are merged together and points located on pixels with intensities lower than a threshold (Intensity-Threshold) are discarded. The remaining points are considered as cell centers and their number corresponds to the searched number of cells in the image. Both Merging-Threshold and Intensity-Threshold were chosen intuitively based on cell sizes and intensities. The algorithm is summarized in Figure 7.

Figure 8(A) depicts the proposed algorithm performance on a synthetic image and Figure 8(B) illustrates its performance on a confocal image of growth plate tissue. Since the method follows the direction of the flow of gradient in each pixel, it was named 'gradient-based flow' (GBF) method.

Selection of vicinity area and initial positions of points

The shape and size of vicinity area (dimensions a and b) were selected to be as similar as possible to the shape and size of the cells in the image. The initial distribution of points on image was also chosen so that at least one point converges to each cell. The most conservative choice is to allocate one point to each pixel. However, to reduce computation time, it is desirable to minimize the number of points as far as possible. For this reason, if prior information of the minimum distance between cell centers is available, a grid of points with a step equal to this minimum distance is recommended. For all the grids with a step lower than this minimum distance, the final result was the same. The grids of points can also be distributed differently in various regions of the images.

Comparison with other methods

To evaluate the performance of our method, it was compared with four other similar existing algorithms developed for segmentation of cells in images with closely packed cells: the IF, the GFT algorithm by Li *et al.* (2008), the original implementation of MS algorithm and the mean shift-based single-pass voting algorithm (Voting) by Qi *et al.* (2012). The IF algorithm was implemented based on the formulation of Esteves *et al.* (2012). The CI for IF algorithm was evaluated using Eq. (4)

$$IF(x, y) = \frac{1}{N}\sum_{i=0}^{N-1}\left[\max_{0\le r\le R_{\max}}\frac{1}{r}\sum_{m=1}^{r} CI(x, y)\right], \qquad (4)$$

where $R_{\max}$ is the maximum radius of the region of support, N is the number of radial directions and $CI(x, y)$ and $IF(x, y)$ are the CI and IF value at point (x, y), respectively. The GFT algorithm was implemented based on the formulation of Li *et al.* (2008). First, the gradient flow was diffused on the image based on an elastic deformable model. Then, through a gradient tracking process and adaptive thresholding, the image was segmented to smaller regions. Finally, the small regions and pale regions were eliminated (Li *et al.*, 2008). The MS algorithm was implemented based on the formulation by Cheng (1995) using a Gaussian kernel. The Voting algorithm was implemented based on the seed detection formulation by Qi *et al.* (2012). The voting image was calculated from the original image and MS algorithm was performed on the thresholded voting image to detect the cell centers.

In order to evaluate the performance of our method in comparison with these four other algorithms, we have first tested all the methods on an image containing one cell type in different resolutions. The original high-resolution image of endothelial cells stained with cell viability assay kit was taken from the VACE fluorescent Gallery[1] . Thereafter, the methods that had provided satisfactory results in low-resolution images were further compared with our method on low-resolution images of growth plate containing three different sizes and shapes of cells (the other methods with poor results on low-resolution images in the first step of evaluation were discarded in the second step because all the images of the second step had low resolution).

For both evaluations, in order to evaluate the precision of our method in comparison with the others, all methods were compared with manual counting. Manual counting was performed by two independent individuals using the *ImageJ cell counter plugin* (National Institutes of Health). Each individual was asked to count the number of cells in each of the three zones of the live and dead channels of the data set. The inter-observer agreement was calculated using Krippendorff's alpha coefficient for the number of cells counted in each zone of live and dead images. The average result from the two users was then used as ground truth for further comparisons.

Evaluation

In the first evaluation, in order to investigate the effect of image resolution on the performance of the methods, the percentage of correctly identified cell centers with respect to manual counting was evaluated for each method for different resolutions of the same image. In the second evaluation, in order to evaluate the accuracy of the methods for low-resolution images with different sizes and shapes of cells, comparisons were made on each zone of the growth plate and for the two channels (live and dead) for 15 confocal images of growth plates obtained with the method detailed in section on 'Tissue Preparation and Image Acquisition'. The absolute relative error with respect to the average of MC result was calculated. The manual cell counting approach was considered as the ground

[1] http://www.ceas3.uc.edu/vace/vfg.html

```
1   Distribute points initially on image
2   for each point P_i
3   Repeat
4   r ← Calculate resultant vector
5   dP ← r*Simulation-Step
6   P_i ← P_i + dP
7       until ||dP|| > Motion-Threshold
8   end for
9   Merge points closer than Merging-Threshold
10  Remove points on pixels with intensity lower than Intensity-Threshold
```

Fig. 7. GBF algorithm.

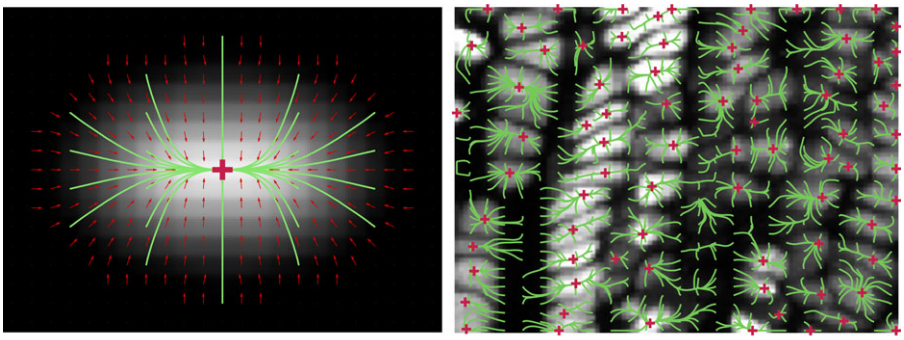

Fig. 8. Point trajectories and detected cell centers using GBF. The plus signs (+) show the detected cell centers.

truth for performance evaluation of automatic methods. The absolute relative error (E_M) was calculated using Eq. (5)

$$E_M = \left| \frac{N_{AC} - N_{MC}}{N_{MC}} \right|, \quad (5)$$

where N_{AC} and N_{MC} are the number of detected cells using automatic counting or MC, respectively.

Results

Parameters setting for the algorithms

For all the methods tested in this paper, the size-dependent parameters were selected based on preliminary estimation of the size and shape of cells and were optimized to give the best result. The parameters used for the VACE fluorescent image to test the effect of resolution are listed in Table 1. In different resolutions, the only parameter that was varied was R, which was a function of image resolution.

For the GBF algorithm, our recommended values for simulation step coefficient is 0.1/R and for minimum point movement is 0.01 × simulation step coefficient. Based on our experimentation, these recommended values worked well for all tested images. Smaller values for these two parameters did not make any significant improvement on the results, although larger values may reduce the accuracy. The merging-threshold and intensity-threshold were the same for all the images in the data set. The merging-threshold was 2 pixels for GFT and GBF algorithms and R for the rest. The intensity-threshold was 30% of maximum for all the methods.

The parameters used for the growth plate fluorescent images are listed in Table 2.

Table 1. Parameters setting for VACE fluorescent image as a function of cell radius (R)

IF		Uniform kernel, cut-off size: 1.5 R, grid step:1
GFT	Filter	Gaussian filter, σ = R, cut-off size: 1.5R
	GFT	$\mu = 0.1$, $\lambda = 0.1$, iteration = 80
MS		Uniform kernel, cut-off size: R, grid step: 1
Voting	Voting	Gaussian kernel, σ = R/6, cut-off size: $r_{min} = 0$ & r_{max} = R, gradient threshold: 20% of max, voting image-threshold: 20% of max
	MS	Uniform kernel, cut-off size: R/1.5, grid step: 1
GBF		Parabolic kernel,α = 1, cut-off size: R, grid step: R

Table 2. Parameters setting for growth plate images as a function of cell radius (R)

IF		Uniform kernel, cut-off size: 1.5 R, grid step: 1, N = 36
GFT	Filter	Gaussian filter, σ = R, cut-off size: 1.5R
	GFT	$\mu = 0.1$, $\lambda = 0.1$, iteration = 80
GBF		Parabolic kernel,α = 1, cut-off size: R, grid step: R

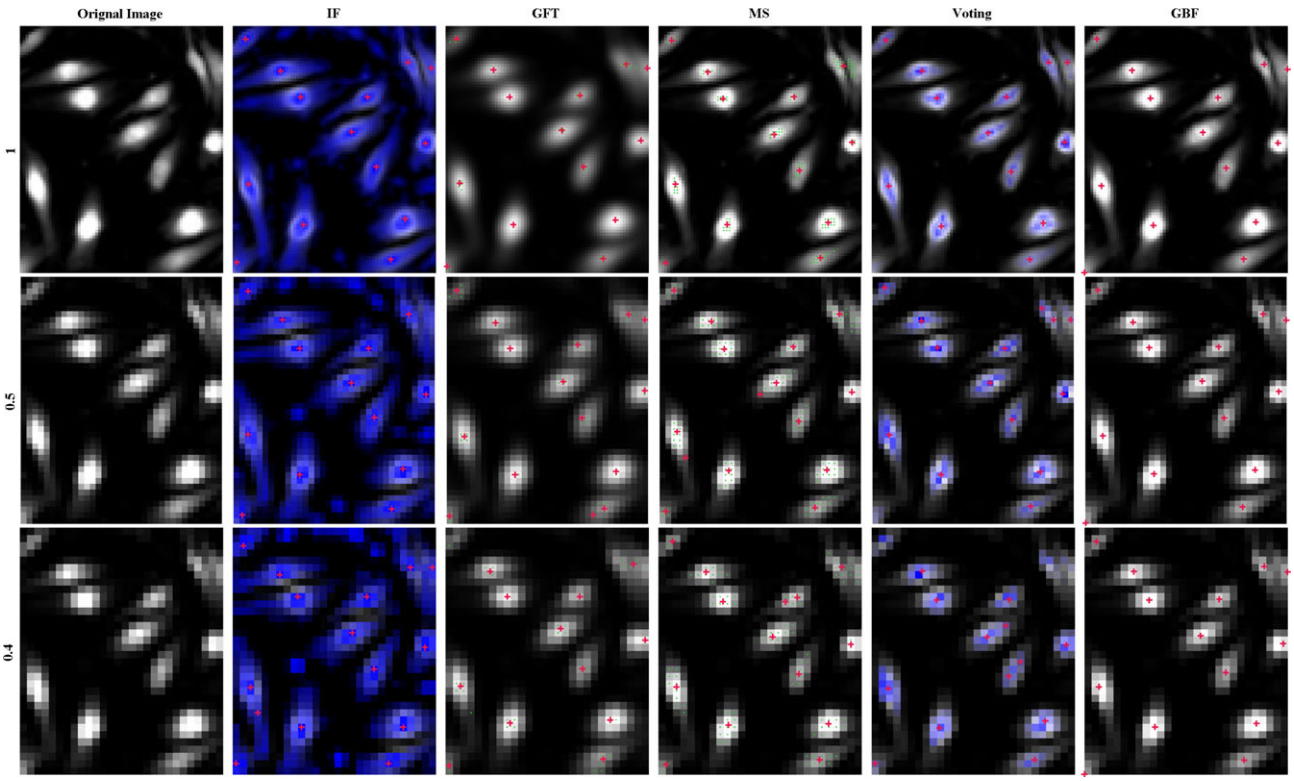

Fig. 9. Effect of image resolution on the performance of each method (IF: Iris Filter; GFT: Gradient Flow Tracking, MS: Mean Shift, Voting: Mean shift-based voting and GBF: Gradient-Based Flow) as a function of resolution with respect to the original resolution.

Interobserver agreement

The calculated Krippendorff's alpha coefficient for the number of cells in different zones of live and dead channels was found to be in the range of 0.96 to 0.98. Based on the calculated Krippendorff's coefficient, a good agreement was found between the counted numbers of cells by the two observers.

Comparison of the performance of the methods on images with different resolutions

Figure 9 shows an example of the performance of IF, GFT, mean shift, voting algorithm and GBF, on the image with single type endothelial cells with three different resolutions taken from VACE database. The intermediate results are also superposed on the original images in terms of blue or green points. The final detected cells are marked with red + symbol. Figure 10 depicts, for each method, the percentage of correctly identified cell centers with respect to the image resolution on the endothelial cells image. As it can be observed from the results, all the above-mentioned algorithms provided very good results in detecting cells in high-resolution images. However, when the resolution of the image was reduced in a way that each cell diameter is about 10 pixels, the performances of mean shift and voting algorithm in identifying the cell centers were reduced 30% and 20%, respectively.

Comparison of the performance of the methods on low-resolution growth plate images containing cells with three different shapes and sizes

Since the MS and the Voting algorithms did not show a good performance on low-resolution images, only the IF, GFT and GBF algorithms were compared in this second evaluation. An example of the result of the three methods is presented in Figure 11 for images of the three growth plate zones. In Figure 12, the absolute relative errors (E_M) for quantification of live and dead cells in each growth plate zone are presented for the three methods showing their best performance in low-resolution images. The average absolute relative errors (mean ± SD%) of our method (GBF) for live cells with closely packed cell clusters in the hypertrophic zone, proliferative zone and reserve zone were 4.3 ± 3.5%, 4.6 ± 1.9% and 2.7 ± 2 .0%, respectively. Errors were, respectively, 31.1 ± 15.0%, 14.3 ± 5.4% and 9.2 ± 7.3% using the IF-based quantification method and 9.5 ± 5.2%, 27.6 ± 13.3% and 6.1 ± 4.3% for the GFT method for the hypertrophic, proliferative and reserve zones. For dead cell images, absolute relative errors for the three zones were 13.2% ± 25.0%, 9.6% ± 1.1% and 5.0% ± 7.2% in the hypertrophic, proliferative and reserve zones, respectively, using our GBF method whereas they were 18.0% ± 28.2%, 21.1% ± 17.0% and 22.6% ± 27.1% using the IF

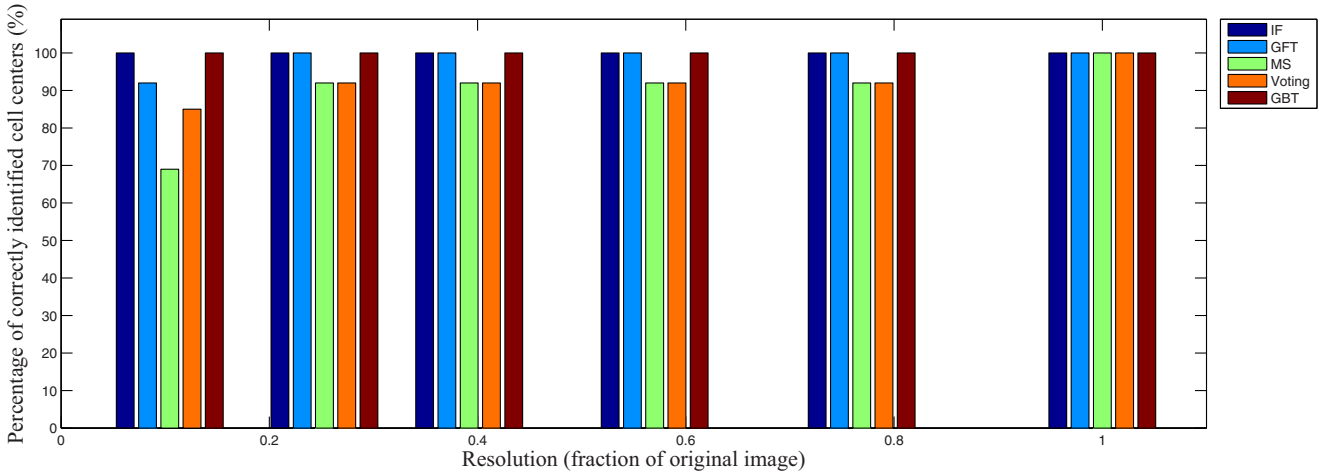

Fig. 10. Effect of decreasing image resolution on the number of correctly identified cell centers.

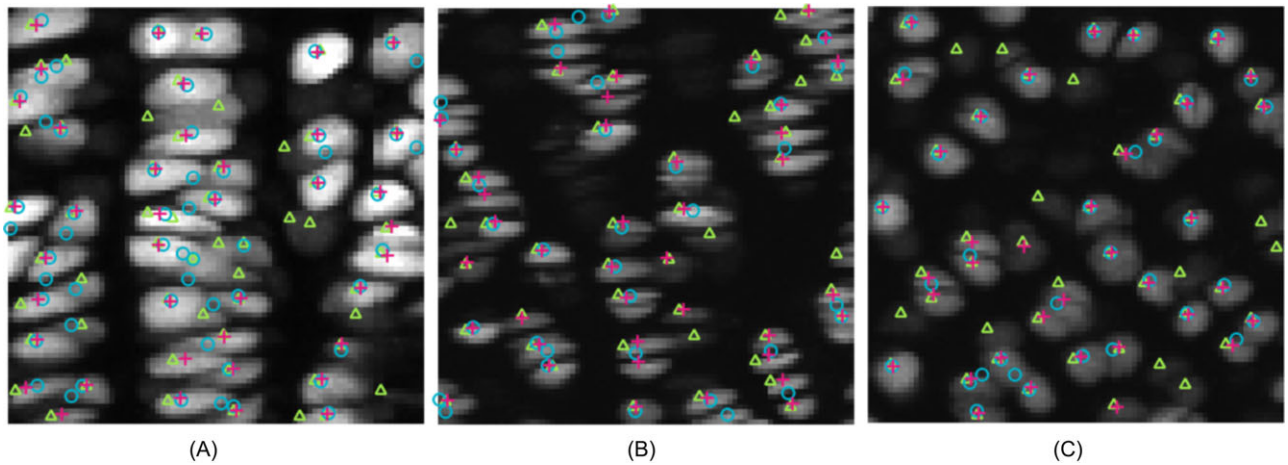

Fig. 11. Cell detection results using GBF (+), GFT (Δ) and IF (o) methods.

and 64.2% ± 29.1%, 53.7% ± 24.5% and 42.4% ± 27.6% using the GFT method.

Discussion

In this paper, a method for quantification of cell viability in low-resolution confocal images of growth plate based on gradient flow tracking of the image was introduced and evaluated. Growth plate has three different zones: *reserve*, *proliferative* and *hypertrophic* (Ballock & O'Keefe, 2003), in which the shape, size, arrangement and density of cells are different (Wongdee *et al.*, 2012). Therefore, the algorithm had to be robust enough to detect cells with different shapes and sizes from the three zones. Moreover, using the current microscopy systems, taking an image spanning the three zones of growth plate, results in a low-resolution image. As a result, the developed algorithm was required to perform well on low-resolution images.

GBF, IF and GFT methods perform well on low-resolution images

Several methods had previously addressed the problem of closely packed cells; however, most of them do not identify cell centers properly in low-resolution images when cells are closely packed such as the growth plate images introduced in this paper. Since most of these methods work properly in identifying cell centers in images containing closely packed cells in the literature, in this paper, we decided to compare our new method with several state-of-the-art methods on a simple image with one cell type but in different resolutions. So that we can only study the effect of image resolution on the performance of each method. Our method (GBF) was compared with the IF, a CI filter, the GFT method of Li *et al.* (2008) as well as the mean shift (Cheng, 1995) and mean shift-based single voting algorithms by Qi *et al.*, 2012. The IF method is similar to sliding band filter, which has been shown to be effective

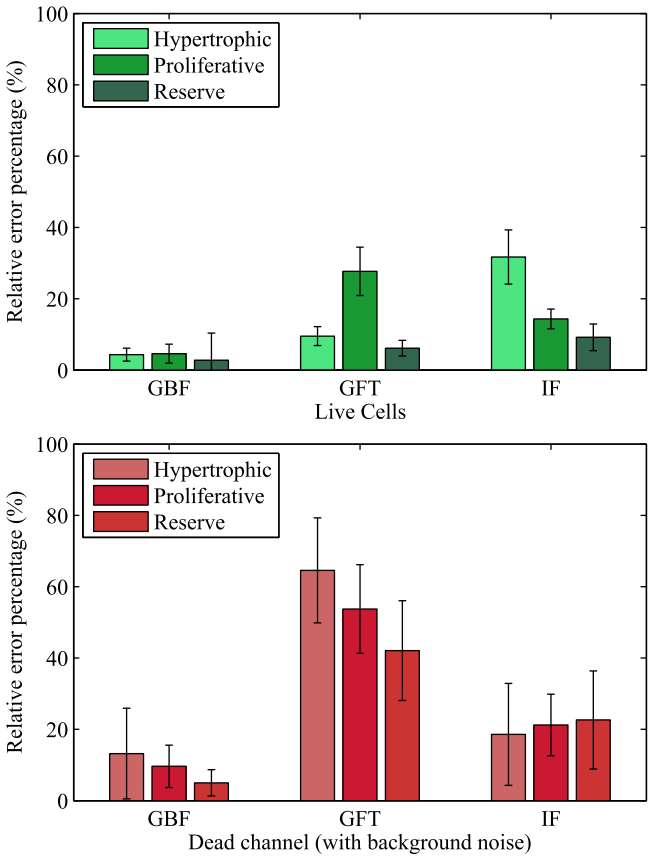

Fig. 12. Average absolute relative error EM in the number of cells per zone using GBF, IF and GFT for live and dead channels.

in quantifying the number of closely packed cells in images with similar cell size (Sui & Wang, 2013). The only difference between the IF and the sliding band filter is that sliding band filter does not take into account the information in the center of cells, which is noisy in some cases. Since in our confocal fluorescent images, the centers of cells are not noisy (due to the fluorochrome type and imaging method), our proposed method (GBF) was only compared to IF. Although IF algorithm works well on low-resolution images, they are not designed to find cells with different sizes and shapes. Also, to emphasize the difference between our method and the GFT, we have also compared our GBF method with the GFT method. Unlike GFT method, our method does not require a lot of preprocessing and denoising, which in some cases can lead to loss of data. Moreover, because of similarity between our method and the MS algorithm, we have also compared our results with mean shift and a mean shift-based voting method. Both methods worked well for high-resolution images but for low-resolution images containing one cell type (endothelial cell images), they were 30% and 20% less efficient. On images with different cell size and shape (growth plate images), they could not even identify 50% of cell centers correctly (data not shown).

The GBF method performs better than IF and GFT algorithms for the detection of both live and dead cells on low-resolution images

Considering the performance of the three algorithms when comparing the calculated absolute relative errors with respect to MC, it can be observed that GBF provides a better performance than IF and GFT for both live and dead cells in all the three zones of the growth plate. In the hypertrophic and reserve zones, where cells are less close to each other, the GFT has a better performance than IF. However, in the proliferative zone, where cells are closely stacked, the worst performance of GFT was observed. In general, since the GFT method uses the data of one point to calculate the direction of gradient, it is very sensitive to local intensity changes. Thus, to avoid finding several centers for each cell, as a preprocessing step, a Gaussian filter with high kernel is applied to the image for smoothing the texture of cells before implementing gradient diffusion on it. In the cases where cells are too close to each other (distance of 3–4 pixels), they will be merged and, as a result, fewer cell centers will be detected. Hence, both in our method and IF, the average gradient of the vicinity area is used in each point to estimate the direction of gradient, which could explain why these two methods are less dependent on the local intensity changes.

The performance of GBF algorithm is less dependent on the choice of vicinity area in comparison to IF algorithm

In comparison to the IF algorithm, our GBF algorithm is less sensitive to the size of vicinity area and, as a result, by choosing a vicinity area similar to the average size of the cells of the three zones of growth plate, the absolute relative error in the number of detected cells is lower than IF. IF also works well for segmentation of closely packed cells but for cells of similar size. Since growth plate images consisted of cells with various sizes, it was not possible with IF to choose a suitable radius parameter for segmentation of all cells and, consequently, the absolute relative error of the detected number of cells was higher for all the three growth plate zones. In that case, if the parameter for the radius was not large enough in the hypertrophic zone the cells were oversegmented. On the other hand, if the radius was chosen with respect to the size of hypertrophic cells, many smaller cells in the proliferative and reserve zones were not detected. One might speculate that the inefficient performance of the IF algorithm in this paper is a consequence of poor choice of parameters. We therefore ran several experiments using different parameters and the best result was presented and used for comparison in this paper. Also, based on several preliminary tests, if the vicinity area of GBF was chosen much smaller than the cell size, the algorithm could detect several centers for some cells, especially when image of cells were saturated or noisy. Also, if the vicinity area was chosen much larger than the cell size, the algorithm might not identify some of the centers and only detect cell centers with higher intensity at each region of closely packed cells.

Conclusion

The GBF method proposed in this study detects the gradient convergence centers, which can correspond to cell centers by generating and following a gradient-guided streams for a set of initial imaginary points on the image using a mean shift-based algorithm. Although many methods have been previously suggested for segmentation of closely packed cells, several fail to identify cells centers in low-resolution images. Using experimental data, the performance of this algorithm was found better than the two other similar algorithms, which also work well in low-resolution images (IF and GFT). This developed GBF method will be useful for quantification of viability in confocal images of tissue sections or cells.

Acknowledgement

This research was supported by Canada Research Chair in Mechanobiology of the Paediatric Musculoskeletal System (I.V.), the CIHR/MENTOR program, Sainte-Justine UHC Foundation and Foundation of Stars (R.K.).

References

Ballock, R.T. & O'Keefe, R.J. (2003) Physiology and pathophysiology of the growth plate. *Birth Defects Res. C Embryo Today*. **69**, 123–143.

Bernardis, E. & Yu, S. (2010) Finding dots: segmentation as popping out regions from boundaries. In *Proceedings of the IEEE Comp. Vis. Pattern Rec*. IEEE, San Francisco, CA.

Chan, Y.-K., Pai, P.-Y., Liu, C.-C., Wang, Y.-S., Li, C.-W. & Wang, L.-Y. (2012) Fluorescence microscopic image cell segmentation. *Int. J. Fut. Comput. Comm.* **1**, 72–75.

Cheng, Y. (1995) Mean shift, mode seeking, and clustering. *IEEE T. Pattern Anal.* **17**, 790–799.

Collins, R.T. (2003) Mean-shift blob tracking through scale space. In *Proceedings of the IEEE Comp. Vis. Pattern. Rec*. IEEE, Madison, WI.

Esteves, T., Quelhas, P., Mendonça, A.M. & Campilho, A. (2012) Gradient convergence filters and a phase congruency approach for in vivo cell nuclei detection. *Mach. Vision. Appl.* **23**, 623–638.

Gantenbein-Ritter, B., Sprecher, C.M., Chan, S., Illien-Jünger, S. & Grad, S. (2011) Confocal imaging protocols for live/dead staining in three-dimensional carriers. *Mammalian Cell Viability*. Springer, Berlin, Heidelberg.

Godfrey, W.L., Hill, D.M., Kilgore, J.A., *et al.* (2005) Complementarity of flow cytometry and fluorescence microscopy. *Microsc. Microanal.* **11**, 246–247.

Gonzalez, R.C. & Woods, R.E. (2002) *Digital Image Processing*. 2nd edn. Prentice Hall, Upper Saddle River, NJ

Guan, P.P. & Yan, H. (2011) Blood cell image segmentation based on the Hough transform and fuzzy curve tracing. In *Proceedings of the Int. Conf. Mach. Learn and Cyber*. IEEE, Guilin.

Kobatake, H. & Hashimoto, S. (1999) Convergence index filter for vector fields. *IEEE T. Image Process.* **8**, 1029–1038.

Li, G., Liu, T., Nie, J., *et al.* (2008) Segmentation of touching cell nuclei using gradient flow tracking. *J. Microsc.* **231**, 47–58.

Malpica, N., Ortiz de Solorzano, C., Vaquero, J.J., Santos, A., Vallcorba, I., Garcia-Sagredo, J.M. & Pozo, F.D. (1997) Applying watershed algorithms to the segmentation of clustered nuclei. *Cytometry* **28**, 289–297.

Nam, D., Mantell, J., Bull, D., Verkade, P. & Achim, A. (2012) Segmentation and analysis of insulin granule membranes in beta islet cell electron micrographs. In *Proceedings of the European Sig. Process. Conf.* IEEE, Bucharest, Romania.

Park, J.C., Hwang, Y.S. & Suh, H. (2000) Viability evaluation of engineered tissues. *Yonsei Med. J.* **41**, 836–844.

Parvin, B., Yang, Q., Han, J., Chang, H., Rydberg, B. & Barcellos-Hoff, M.H. (2007) Iterative voting for inference of structural saliency and characterization of subcellular events. *IEEE T. Image Process.* **16**, 615–623.

Qi, X., Xing, F., Foran, D.J. & Yang, L. (2012) Robust segmentation of overlapping cells in histopathology specimens using parallel seed detection and repulsive level set. *IEEE T. Biomed. Eng.* **59**, 754–765.

Quelhas, P., Marcuzzo, M., Mendonça, A.M. & Campilho, A. (2010) Cell nuclei and cytoplasm joint segmentation using the sliding band filter. *IEEE T. Med. Imaging.* **29**, 1463–1473.

Spaepen, P., De Boodt, S., Aerts, J.-M. & Vander Sloten, J. (2011) Digital image processing of live/dead staining. In: *Mammalian Cell Viability*. Humana Press, New York City.

Stoddart, M.J. (2011) Cell viability assays: introduction. In: *Mammalian Cell Viability*. Humana Press, New York City.

Sui, D. & Wang, K. (2013) A counting method for density packed cells based on sliding band filter image enhancement. *J. Microsc.* **250**, 42–49.

Wongdee, K., Krishnamra, N. & Charoenphandhu, N. (2012) Endochondral bone growth, bone calcium accretion, and bone mineral density: how are they related? *Niger. J. Physiol. Sci.* **62**, 1–9.

Xiong, G., Zhou, X., Ji, L., Bradley, P., Perrimon, N. & Wong, S. (2006) Segmentation of drosophila RNAi fluorescence images using level sets. In *Proceedings of the Int. Conf. Img. Proc*. IEEE, Atlanta, GA.

Yang, X., Li, H. & Zhou, X. (2006) Nuclei segmentation using marker-controlled watershed, tracking using mean-shift, and Kalman filter in time-lapse microscopy. *IEEE Trans. Circuits. Syst. I Regul. Pap.* **53**, 2405–2414.